NASA Technical Memorandum 4796

Finite-Element Analysis of a Mach-8 Flight Test Article Using Nonlinear Contact Elements

W. Lance Richards

June 1997

NASA Technical Memorandum 4796

Finite-Element Analysis of a Mach-8 Flight Test Article Using Nonlinear Contact Elements

W. Lance Richards
Dryden Flight Research Center
Edwards, California

National Aeronautics and
Space Administration

Office of Management

Scientific and Technical
Information Program

1997

ABSTRACT

A flight test article, called a glove, is required for a Mach-8 boundary-layer experiment to be conducted on a flight mission of the air-launched Pegasus® space booster. The glove is required to provide a smooth, three-dimensional, structurally stable, aerodynamic surface and includes instrumentation to determine when and where boundary-layer transition occurs during the hypersonic flight trajectory. A restraint mechanism has been invented to attach the glove to the wing of the space booster. The restraint mechanism securely attaches the glove to the wing in directions normal to the wing/glove interface surface, but allows the glove to thermally expand and contract to alleviate stresses in directions parallel to the interface surface. A finite-element analysis has been performed using nonlinear contact elements to model the complex behavior of the sliding restraint mechanism. This paper provides an overview of the glove design and presents details of the analysis that were essential to demonstrate the flight worthiness of the wing-glove test article. Results show that all glove components are well within the allowable stress and deformation requirements to satisfy the objectives of the flight research experiment.

INTRODUCTION

Preparations are currently underway for a flight experiment that will acquire data necessary to validate boundary-layer transition prediction methods for hypersonic flight conditions. Success of the flight experiment depends on the design and development of a flight test fixture, called a glove, which can provide a smooth, three-dimensional, structurally stable, aerodynamic surface from which detailed information regarding the atmospheric flight environment to a maximum of Mach 8 could be obtained.

A flight test article has been designed, analyzed, manufactured, and installed on the wing of the air-launched Pegasus® (Orbital Sciences Corporation, Fairfax, Virginia) space booster. Figure 1 shows the geometry of the booster and the location of the glove for the boundary-layer experiment. The Pegasus® is a multistaged, air-launched rocket designed to place small payloads into low Earth orbit. The booster follows a predetermined trajectory designed for a particular payload requirement. For a typical mission, the booster separates from the carrier aircraft at Mach 0.8 and an altitude of approximately 13,000 m. The booster descends for 5 sec before the first stage ignites. After approximately 70 sec, the vehicle has accelerated to Mach 8 and an altitude of approximately 61,000 m. The glove experiment concludes as the first stage burns out and is jettisoned and second-stage ignition occurs.

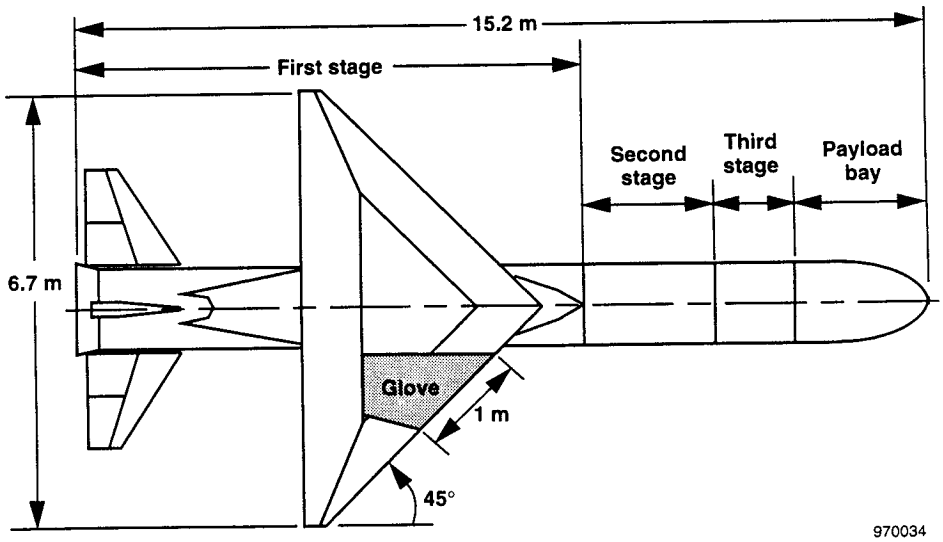

Figure 1: Plan view of Pegasus® space booster with glove.

Figure 2 shows a photograph of the Pegasus® space booster mounted under the wing of the NASA B-52 airplane, which was the original carrier aircraft. The booster has recently been air-launched from a modified L-1011 aircraft. Details of previous research experiments conducted on the Pegasus® booster have previously been provided.[2,3] Plans for future studies have also been previously presented.[4]

A comprehensive structural test and analysis program has been successfully completed to validate the integrity of the complex glove design.[5,6] Complexity of the design stemmed from the use of a nonlinear restraint mechanism that attaches the glove to the wing of the space booster. The restraint mechanism securely attaches the glove to the wing in directions normal to the wing/glove interface surface, but allows the glove to thermally expand and contract to alleviate stresses in directions parallel to the interface surface. This design allows the glove to maintain a geometrically stable shape, reduces the thermal stress in the glove to acceptable levels, and results in safe and efficient structural performance.

A finite-element analysis was performed using nonlinear contact elements to model the complex behavior of the sliding restraint mechanism. This paper provides an overview of the glove design and presents details of the finite-element analysis, which included the use of nonlinear contact elements to accurately predict the structural response of the test article prior to flight. Results from the analysis show that all glove components are well within the allowable stress and deformation requirements to satisfy experiment objectives.

GLOVE DESIGN

Figure 3 shows a top view of the glove, the rigid attachment at the inboard leading edge, and a cross-sectional view of the glove. The test surface has a plan view area of approximately 1 m^2. Ceramic tile and ablative-coated aerodynamic fairings[5] were used to blend the metallic portion of the glove to the existing Pegasus® wing. Details of

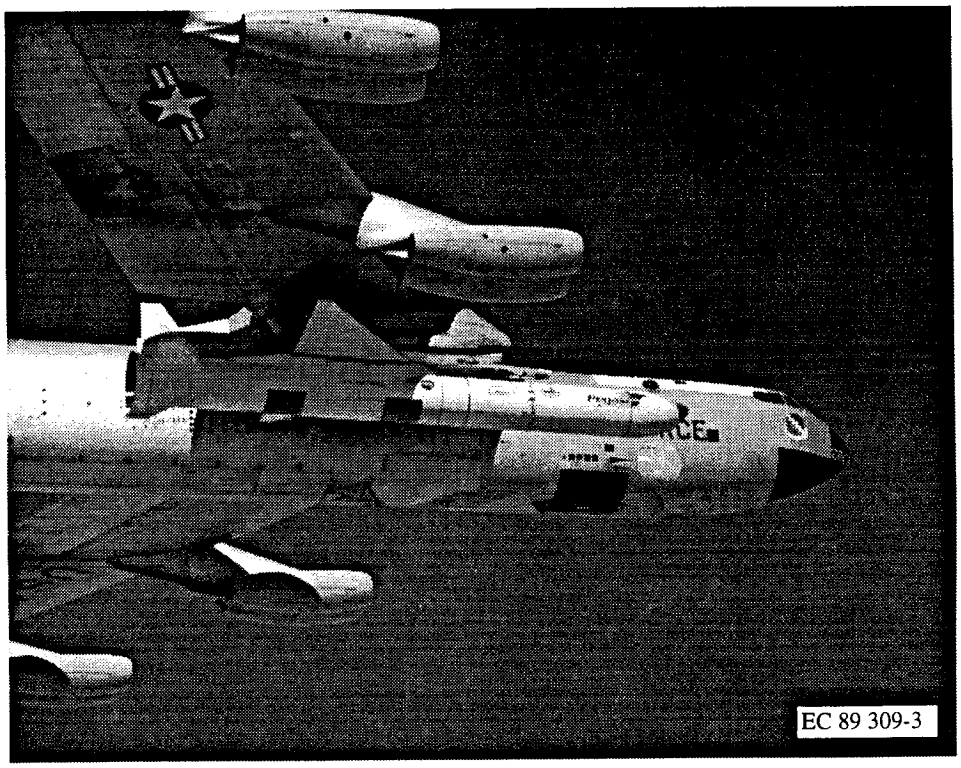

Figure 2: Pegasus® space booster mounted under the wing of the B-52 aircraft.

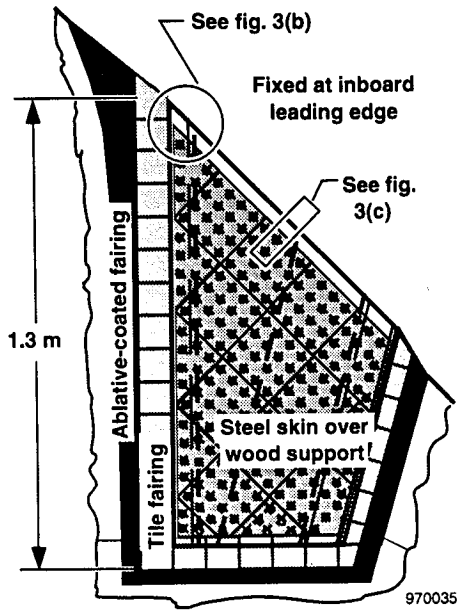

(a) Plan view.

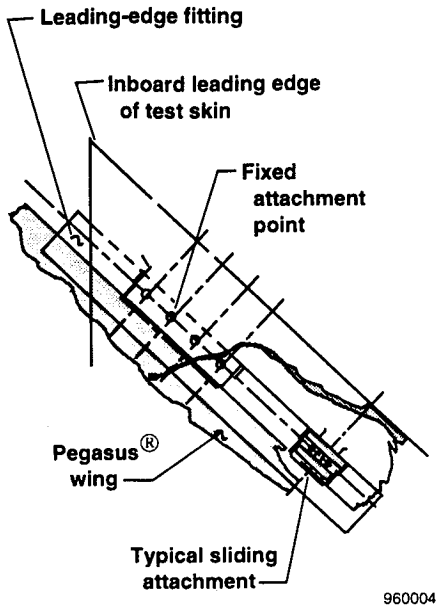

(b) Glove leading-edge detail.

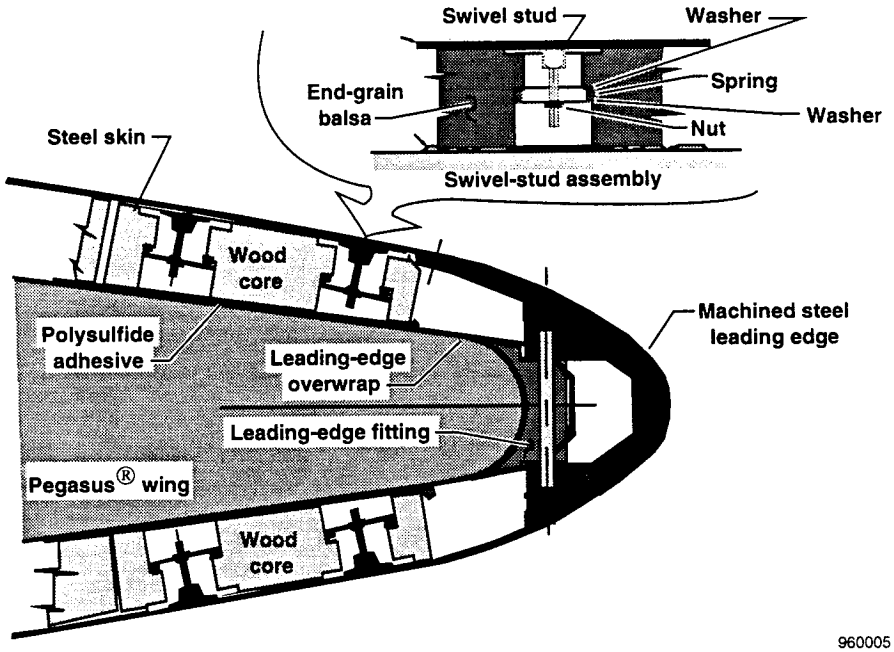

(c) Glove internal assembly.

Figure 3: Glove assembly.

the design process, which consisted of aerodynamic heating analysis, thermal analysis, structural analysis, and small-scale laboratory testing, have been published.[5] This process resulted in a glove design with a relatively thin metallic outer skin and a large leading-edge heat sink (fig. 3(c)) to accommodate the extreme stagnation-point heating rates during flight.

Preliminary analysis showed that if the glove was rigidly constrained during the hypersonic flight experiment, then the thermal stresses produced by aerodynamic heating would cause the thin skins to buckle, or the rigid attachments to yield, or both. Thermal expansion and contraction capability was, therefore, a critical requirement in the glove design. This requirement was satisfied by two means: the thick leading edge was rigidly fixed at a single point only (fig. 3(b)), and the thin metallic skin was allowed to freely expand over a balsa wood support foundation during heating. The preliminary design constrained the movement of the glove in the direction normal to the Pegasus® wing leading edge; however, movement in the direction parallel to the Pegasus® wing leading edge was allowed by a series of sliding attachments. The rigid attachment of the glove (fig. 3(b)) forced all thermal expansion of the glove aft and spanwise parallel to the leading edge. The design ensured glove dimensional stability at the leading edge where boundary-layer transition is the most sensitive to moldline shape.

Figure 3(c) shows a detailed cross-sectional view of the glove attached to the Pegasus® wing at the leading edge. The metallic test skin was attached to a balsa wood support surface that was preshaped and bonded to the Pegasus® wing (fig. 3(c)). The design process used to define the aerodynamic shape of the glove has previously been described.[7] The thin skin was attached to the contoured balsa wood surface using a series of spring-loaded swivel studs spaced approximately 6.35 cm apart. These studs were designed to hold the skin securely to the surface while allowing the skin to expand thermally with only a small resistance caused by sliding friction. Each stud is bonded to the inner surface of the glove skin with high-temperature epoxy. An initial preload is applied through the spring to react against aerodynamic forces expected during the flight experiment.

FINITE-ELEMENT ANALYSIS

Figure 4 shows the top, outboard, forward, and isometric views of the three-dimensional glove model, which was generated using MSC/NASTRAN (Version 68).[8] The fixed attachment point is located at the inboard end of the leading-edge mass (fig. 3(b)). This section describes the elements, analysis cases, loads, boundary conditions, and the solution strategy employed in the nonlinear analysis.

Description of Elements

The model consists of 3777 hexahedron elements, 187 pentahedron elements, and 1194 nonlinear contact-friction elements, resulting in a total of 7500 degrees of freedom. This section describes the types of elements used in the non- linear analysis.

Solid Elements

The massive leading-edge heat sink was modeled with solid, linear, isoparametric elements to incorporate the severe, spatially varying temperature distributions in all three dimensions: radially (through the thickness of the leading edge), circumferentially (around the leading-edge radius), and in the spanwise direction (parallel to the leading edge). Figure 5 shows the reference system. The radial and circumferential temperature variations at the leading edge were produced by severe stagnation-point heating during hypersonic flight. Several layers of isoparametric elements were needed in these directions to adequately define the nonlinear temperature distribution produced by the aerodynamic heating at the leading edge.

Severe temperature gradients also occurred in the spanwise direction because the structurally stiffened attachment points, referred to as bosses (fig. 5), were located at several locations behind the leading edge to secure the glove to the Pegasus® wing. These bosses produced large discontinuities in thermal capacitance that resulted in the temperature variations in the spanwise direction.

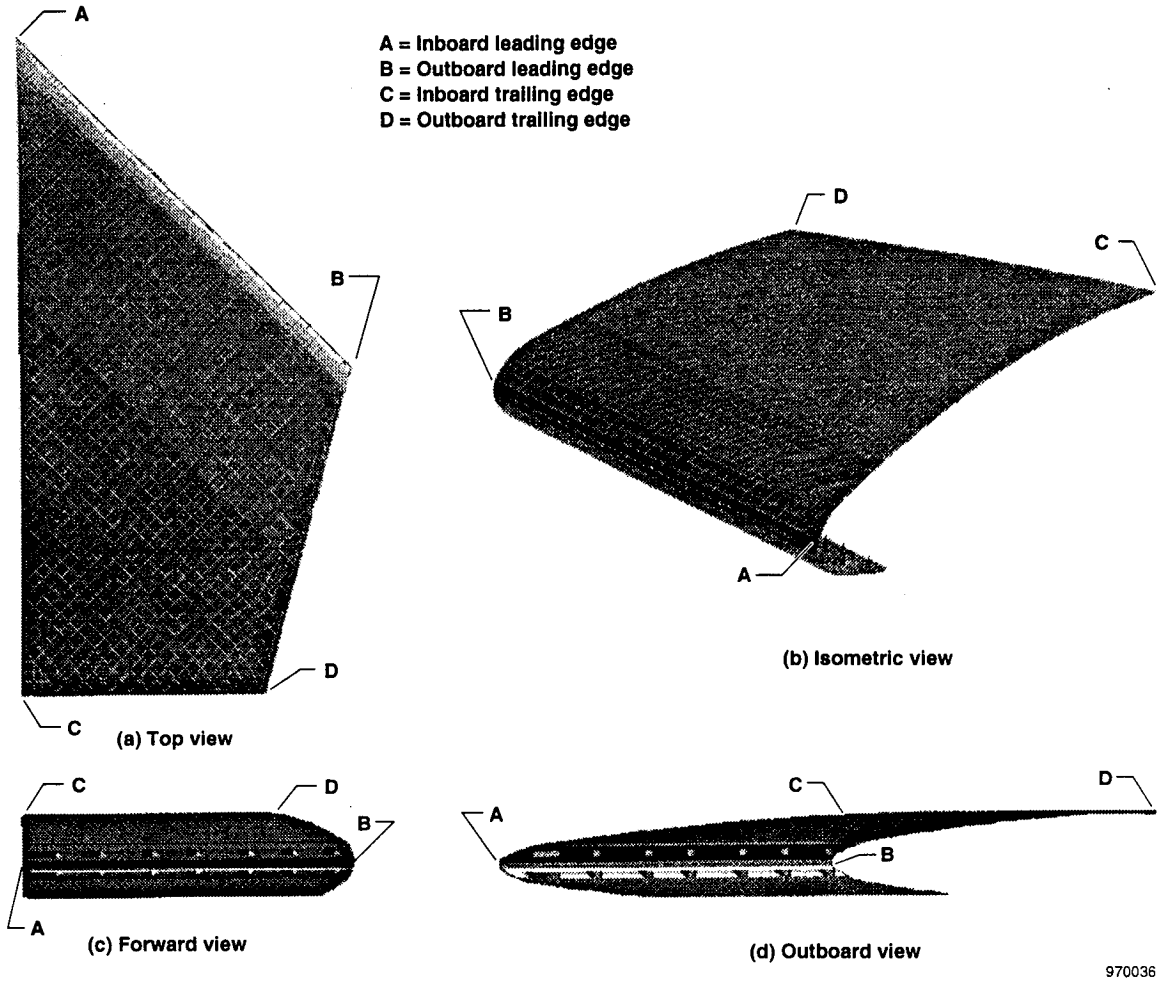

Figure 4: Finite-element model.

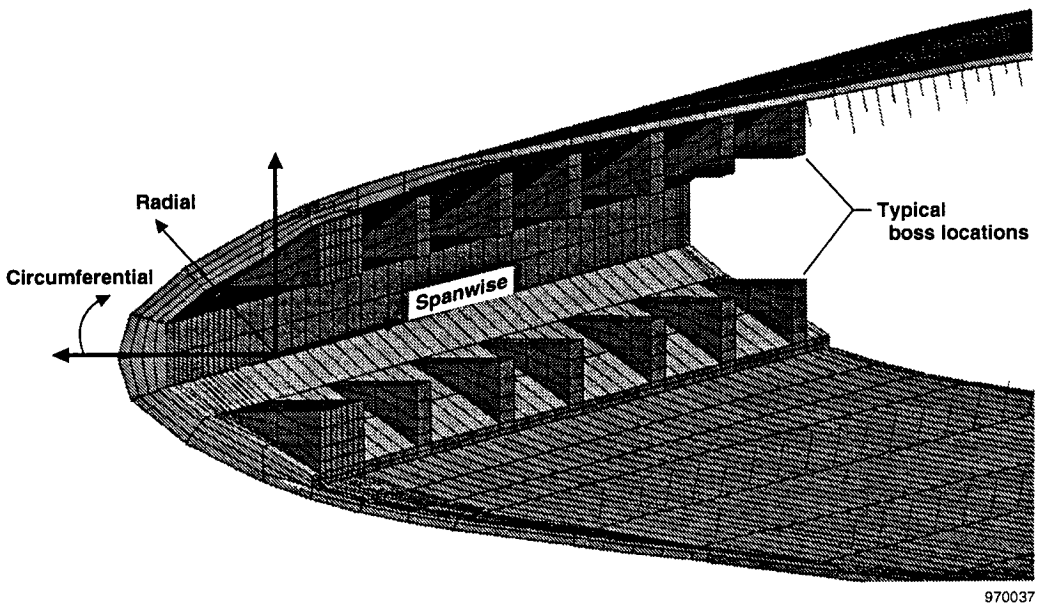

Figure 5: Model detail showing boss locations.

Solid elements were also required in the analysis because of their ability to model the irregular surface topology existing behind the leading edge at the boss locations. To ensure element compatibility, particularly at the interface boundary between the thick and thin regions of the structure, the entire thin skin was also modeled with solid elements. Hexahedron brick-type elements were used wherever possible, and pentahedron wedge-type elements were judiciously used in areas of especially irregular surface geometry.

Although solid elements were selected to model both the thick and thin regions of the structure, it was recognized that solid elements, which are better suited for plane-strain type problems, were not the ideal choice for modeling the thin skin. Therefore, preliminary studies were performed to quantify the reduced computational accuracy in using solid elements to model plane-stress and buckling-critical areas on the glove. In these studies, flat-plate models were constructed with four-noded plate elements and eight-noded solid elements. These models were subjected to large compressive in-plane forces at the panel boundaries, and the critical buckling values were determined for successive refinements in the element mesh. The critical eigenvalues computed from finite-element analysis were compared to analytical solutions based on Timoshenko plate theory.[9] The results showed that the use of solid elements produced a 2.5–percent increase in stiffness compared with similar models constructed with plate elements. When the final glove models were constructed and the fully three-dimensional thermal loads were applied to the glove, the membrane forces produced in the thin skin were determined to be well below critical values. Therefore, the additional stiffness provided by the solid elements was not an issue. The choice of the solid elements to model the glove was the best compromise between the many competing modeling requirements.

Nonlinear Contact Elements With Friction

The element used to model the contact surface between the metallic thin skin and the balsa wood is called an "adaptive gap" element in MSC/NASTRAN.[10] The gap element simulated point-to-point frictional contact and used an adaptive solution procedure based on the penalty method.[10] Initial penalty values were defined prior to the analysis run and were automatically updated during the solution process based on the penetration of the contacting surfaces. The initial penalty value was increased by one order of magnitude if the surface penetration was greater than the user-specified amount. Conversely, the penalty value was automatically decreased by an order of magnitude if the penetration was less than a user-specified amount. The lower and upper bounds of the penalty values were also limited during the analysis. Both static and kinetic friction were considered in the formulation of the element.

The contact surfaces were meshed to ensure that a node was located at each of the 270 swivel-stud assemblies in the balsa wood support system. Each assembly was represented by a gap element that was defined by a pair of noncoincident nodes (similar in geometry to a rod element). Figure 6 shows a schematic of the noncoincident gap element with three possible conditions. The noncoincident gap elements allowed the specification of 1) a closed stiffness, k_w, for the condition when the two surfaces were in contact and resisted by static friction, μ_s; 2) a frictional stiffness that represented the slip forces produced when the surfaces were in contact and resisted by kinetic friction, μ_k; and 3) an open stiffness, k_s, when the surfaces exceeded an initial preload and had separated. In addition to the noncoincident gap, the element can also be defined, similar to a zero-length element, by a pair of coincident nodes. All parameters described above, except k_s, can be specified for the so-called "coincident" gap elements.

Initially, only noncoincident gaps elements, which represented the swivel-stud assemblies, were used in the analysis to avoid the excessive computational expense associated with these nonlinear elements. Further studies showed, however, that coincident gap elements were also required to provide stiffness on the contact surface and prevent unrealistic penetration of the thin skin into the balsa wood substructure. Coincident gap elements were added on the contact surface at all other degrees of freedom where swivel-stud assemblies were not present. Preliminary studies showed that without the coincident contact elements, the buckling resistance of the thin skin was not realistically modeled, causing spurious mode shapes to develop because of buckling.

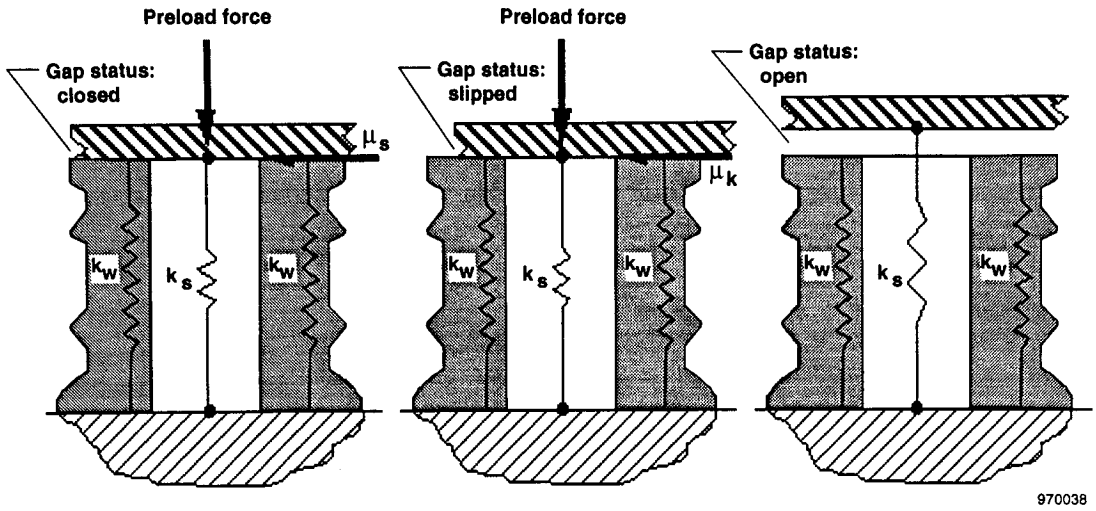

Figure 6: Nonlinear gap elements.

Analysis Cases

In a preliminary analysis, a single time in the trajectory was initially analyzed near the end of the boundary-layer experiment to provide what was assumed as a "worst-case" design condition. Because the first stage of the Pegasus® booster begins to burn out at approximately 69 sec after launch, this time was initially selected for the preliminary analysis. A more rigorous and quantitative analysis later showed, however, that the worst-case condition in the glove will not occur at a single time in the trajectory and that multiple analysis cases were necessary to capture this condition.

Figure 7 shows predicted temperature time histories at the thick leading edge and the thin skin approximately 10 cm in the direction normal to the leading edge of the glove. This figure shows how radically the temperature

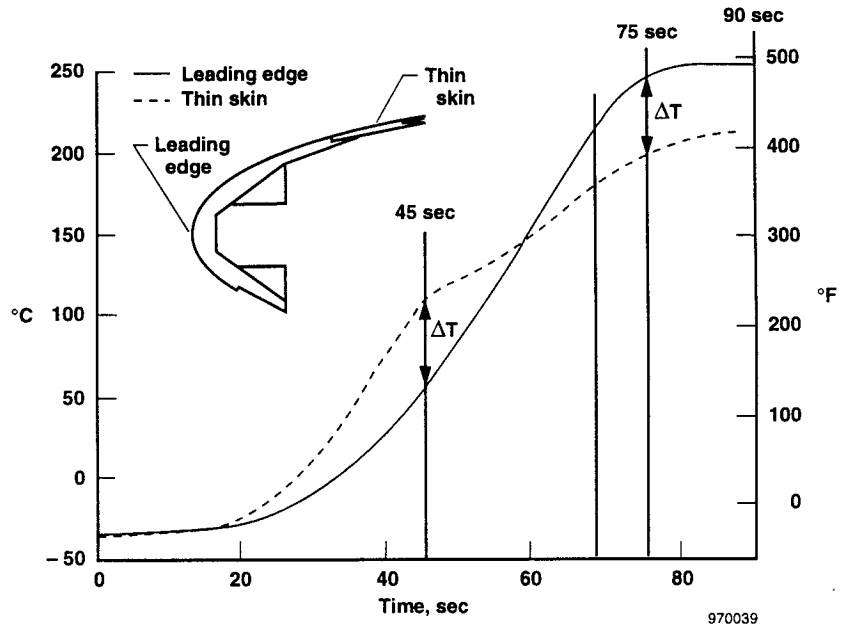

Figure 7: Analysis cases for structural analysis.

differences (and consequently the thermal stresses) can vary over the glove during the course of the trajectory. Approximately 10 analysis cases between 25 and 90 sec were analyzed to ensure that a truly worst-case design in the transient profile was considered. Results from these cases confirmed that maximum thermal stresses in the glove occurred at a flight profile time between 45 and 90 sec. Accordingly, analysis cases discussed in this paper are focused at four critical times in the trajectory: 45, 69, 75, and 90 sec. Times of 45 and 75 sec correspond to the points at which the thermal gradient between the thick and thin regions was the most extreme (fig. 7). As mentioned earlier, a profile time of 69 sec is when first-stage burnout initiates and is the time that was originally chosen for preliminary analyses. At 90 sec, second-stage ignition has occurred and reflects a condition well beyond the conclusion of experiment.

Load and Boundary Conditions

During the flight experiment, the glove will experience a combination of loads from external and internal sources. The external loads chiefly pertain to the aerodynamic loads imparted to the glove (in the form of pressures) as the rocket, to which the glove is mounted, traverses through the atmosphere at increasing hypersonic speeds. To counteract these aerodynamic loads, the thin skin areas of the glove are preloaded mechanically to secure the glove to the Pegasus® wing. These preloads are referred to as "mechanical loads."

In addition, the glove will experience significant thermal loading (in the form of increased temperatures) caused by aerodynamic heating, which increases with the square of the speed. These thermal loads are highly nonuniform, especially near the stagnation region of the glove. Large thermal stresses develop at the boundary restraints between the glove and the Pegasus® wing as the glove attempts to expand and contract with the increased variation in temperature. This section describes how the mechanical, thermal, and aerodynamic loads, as well as the boundary conditions, were modeled in the finite-element analysis.

Mechanical Loads

Mechanical loads were applied in directions normal to the exterior surface of the glove at each of the 210 noncoincident gap element locations (fig. 6). The mechanical loads represented a 110-N initial preload to which each of the swivel-stud mechanisms were subjected when the glove was assembled and attached to the Pegasus® wing. These preload forces were designed to resist against the aerodynamic forces predicted to occur during the experiment.

Thermal Loads

The transient temperature distributions on the glove were determined by the aerodynamic heating and thermal analysis discussed in a previous publication.[6] The temperature distributions at a given trajectory time were mapped onto the structures model so that a unique temperature value was assigned to every node in the model. The code determined the thermal strain at each node by multiplying the coefficient of thermal expansion of the material by the difference between the prescribed nodal temperature and the initial reference temperature. Temperature dependency of the glove material properties were considered in the analysis. The calculated temperature distribution varied considerably over the glove, depending on the time in the trajectory being analyzed. For example, the temperature distribution at 69 sec varied from approximately 400 °C at the inboard end of the leading edge to approximately 65 °C near the trailing edge of the thin skin.

Aerodynamic Loads

In a separate analysis, aerodynamic loads on the glove were determined to only be significant early in the trajectory (achieving a peak at approximately 16 sec after launch and decreasing to zero by approximately 20 sec).

Figure 7 shows that the thermal gradients in the glove are not significant until after approximately 25 sec. The aerodynamic loads were therefore sufficiently decoupled from the thermal structural loads, because they occur at mutually exclusive times in the trajectory. The aerodynamic loads were analyzed separately and will not be addressed in this paper.

Boundary Conditions

The fixed boss at the top inboard area is the only location on the glove rigidly attached to the wing (fig. 3(b)). The degrees of freedom at this location were therefore constrained in the analysis. Initially, the preliminary analysis at 69 sec described above predicted that the attachment of the glove to the leading edge of the wing was well within design allowances. However, the additional analysis cases revealed that the original attachment scheme exceeded design limits at the other times in the flight profile. This problem forced modifications to the design at the inboard restraint and sliding attachments at the leading edge. Originally, the leading edge was prevented from moving in the direction normal to the 45° sweep angle of the wing. This constraint was removed to allow thermal expansion and contraction to occur freely in a direction normal to the leading edge. These design changes allowed greater thermal distortion of the glove outer moldline than previously observed but were essential to reduce thermal stresses in the glove throughout the heating profile.

Nonlinear Solution Procedure

A computationally intensive, nonlinear solution process[9] was used to determine thermal stress and displacements of the glove at each of the analysis cases previously described. Optimization and fine-tuning of the solution strategy were key requirements because of the large number of nonlinear contact elements necessary in the analysis and because friction was considered, which is path dependent. Preliminary studies were performed to define an acceptable compromise between computational efficiency and solution accuracy. This section describes the salient features of the solution process.

User Interface

Prior to the analysis run, important "control" parameters were required as input to define and adjust the algorithm during the solution process. Parameters for the nonlinear process defined advancing schemes, iteration frequency, convergence criteria, load increment and bisection control, and stiffness update strategy.[9] The maximum number of bisections allowed during a load step, stiffness update frequency, divergence and convergence contingencies, and output frequency were also specified. The code permitted some of these parameters to be automatically updated during the solution process to efficiently respond to the nonlinear environment. These parameters were also important because they helped to circumvent numerical difficulties encountered with the contact elements.

Analysis Case Control

The critical loading cases described in an earlier section were divided into separate subcases. The mechanical forces that represented the initial preload on the gap elements were applied separately in the first subcase, and then concurrently applied with thermal load distributions at 45, 69, 75, and 90 sec for the subsequent subcases.

Load Increment and Iteration Strategy

The solution sequence invokes a subincremental algorithm for load application control and stiffness updates. The load application process begins by the calculation of the incremental load to be applied during a given subcase.

Any resulting load from a previous subcase is subtracted from the total load to be applied during the next subcase. For example, if the thermal loads at 45 sec were applied in the previous subcase, and the thermal loads at 69 sec are to be applied in the next subcase, then the resulting loads at 45 sec are subtracted from the loads at 69 sec (at each degree of freedom) to determine the "delta load" to be applied during the next subcase. This delta load, which includes both thermal and mechanical loads, is then further divided by a user-specified value so that only a small increment of the delta load is attempted at a time during the subcase.

An initial load increment of 10 percent was selected for each subcase in the analysis. The Newton-Raphson iteration method was used to achieve equilibrium between the load increment applied and the internal nodal forces produced in the residual structure. During the application of an incremental load, if the code failed to converge efficiently after several iterations, the load increment was automatically bisected and the iteration procedure was resumed from the last converged load condition. This process was repeated until convergence was achieved at each incremental load applied during the subcase. After the entire delta load to be applied during the subcase was completed, the algorithm advanced to the next subcase, and the process was repeated until all the load for all the subcases was applied.

Convergence Criterion

The convergence criterion used in the iteration process was based on the work performed by the incremental load during an iteration, normalized by the total work performed throughout the analysis run. Although displacement and load criteria were also available options, a work criterion option set at 1×10^{-7} (the default value) produced an acceptable balance between solution performance and numerical accuracy.

Adaptive Penalty Values

In addition to checking for convergence during the iteration process, the program also checked to see if any gap elements had changed configuration (for example, from closed to open, or stick to slip) or if unacceptable penetration had occurred at the contact points. If any gap elements changed status, the stiffness matrix was updated to reflect these changes. If unacceptable penetration at the contact points had occurred, then the penalty values for the gap element were automatically adjusted and the iteration process was repeated.

RESULTS AND DISCUSSION

Thermal stresses and displacements of the glove were calculated for multiple analysis cases along the transient-heating profile. This section highlights some of the significant results from the finite-element analysis.

Stress Results

Table 1 shows a summary of the stress results and factors of safety of the most critical components for four of the analysis cases studied. As these results show, all critical glove components are well below the allowable stress with an acceptable margin of safety. The maximum stress result during the trajectory, which is highlighted, was used to determine the component safety factor. As table 1 shows, the maximum stress in various glove components is predicted to occur at different times during the experiment. This result underscores the need for transient analyses; conventional analyses techniques that use static, linear assumptions to simplify the problem would produce erroneous predictions and nonconservative design results.

Figure 8 shows typical output of the program in which the maximum shear stress at 69 sec is mapped on the upper surface of the finite-element model. This figure shows that the area of highest stress at this time occurs at the

Table 1. Stress results.

Glove component	Experiment design case Time, sec				Allowable stress	Factor of safety
	45	69	75	90		
Upper skin						
Max. shear stress, MPa	82	80	84	55	241	2.9
Lower skin						
Max. shear stress, MPa	113	121	117	89	241	2.0
Upper joint						
Max. skin shear stress, MPa	90	96	82	62	241	2.5
Lower joint						
Max. skin shear stress, MPa	136	134	129	97	241	1.8
Leading edge						
Max. shear stress, MPa	120	104	112	118	241	2.0
Boss bearing stress, MPa	48	49	63	66	241	3.7

leading edge in the regions experiencing the highest thermal gradients. The thin skin is relatively stress-free away from the leading edge, especially near the aft end of the glove. Figure 9 shows the maximum shear stress, also at 69 sec, on the lower surface of the model. The results from this figure show that the thin skin is again relatively stress-free away from the leading edge because of the use of nonlinear contact elements.

Deformation Results

The contact elements were critical in the modeling of the expansion and contraction of the thin skin during the severe temperature environment expected during flight. Figure 10 shows the thermal expansion of the glove at 69 sec. (Displacements are magnified by 100 times to show detail.) This figure shows how the gaps have slipped during the trajectory to significantly reduce the thermal stress in the thin skin. For comparison purposes, the same model was also used in a linear finite-element solution to determine the effect of not updating the contact elements during the application of the thermal load. Results from the linear solution showed that thermal expansion was not permitted to this degree, and von Mises stress approaching twice the yield stress of the thin skin material was predicted.

Figure 11 graphically shows the leading-edge distortion at the four critical times analyzed in the heating profiles. This figure also shows why a transient structural analysis was required. The 69-sec deflection, initially assumed as the worst-case condition for the preliminary design, appears the most benign of the four cases studied. The center leading edge thermally distorts inward (toward the Pegasus® wing) at 45 sec in the profile. This phenomenon is consistent with figure 7, which shows the thick leading edge much lower in temperature than the thin skin. At 69 sec, the stagnation heating at the leading edge has forced the leading-edge deflection through its initial undeformed shape. At 75 sec, the thermal gradient between the leading edge and thin skin has caused a displacement nearly equal in magnitude and opposite in sign to the displacement at 45 sec. At 90 sec, the displacement has reached its maximum of 0.30 mm.

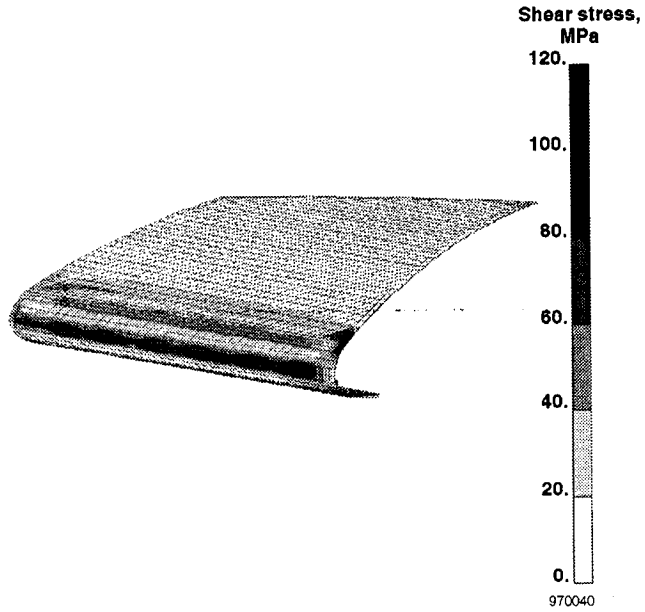

Figure 8: Maximum shear stress at 69 sec.

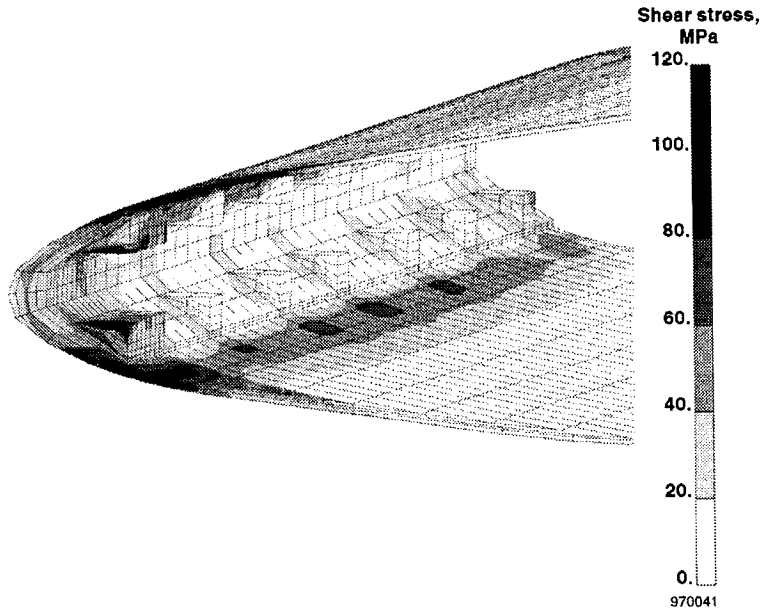

Figure 9: Maximum shear stress on inner surface of lower glove skin at 69 sec.

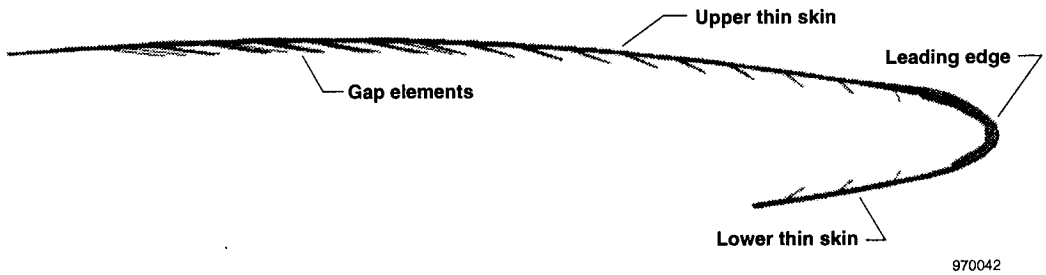

Figure 10: Nonlinear gap element displacements at 69 sec (magnified 100 times).

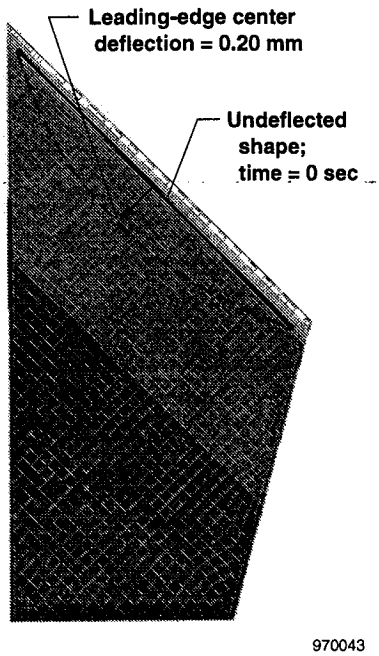

(a) Leading-edge deflection at 45 sec.

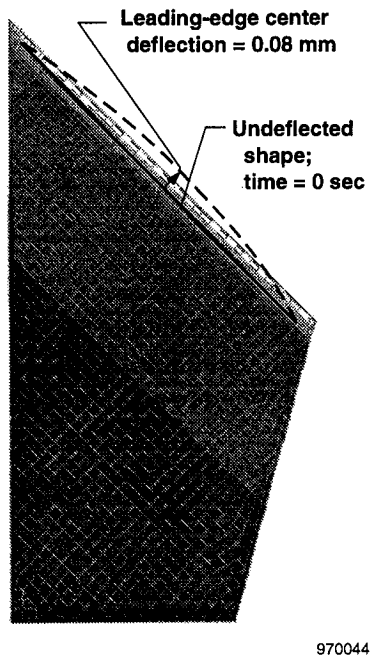

(b) Leading-edge deflection at 69 sec.

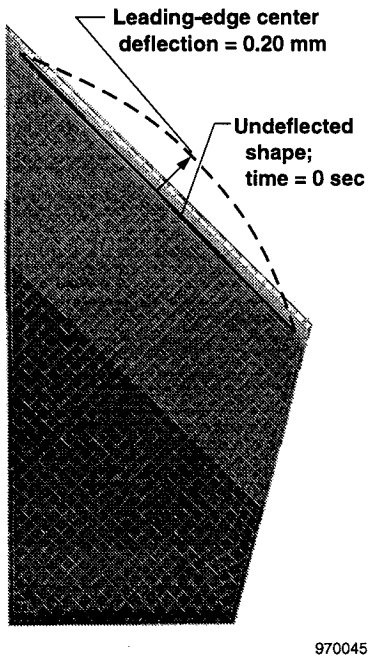

(c) Leading-edge deflection at 75 sec.

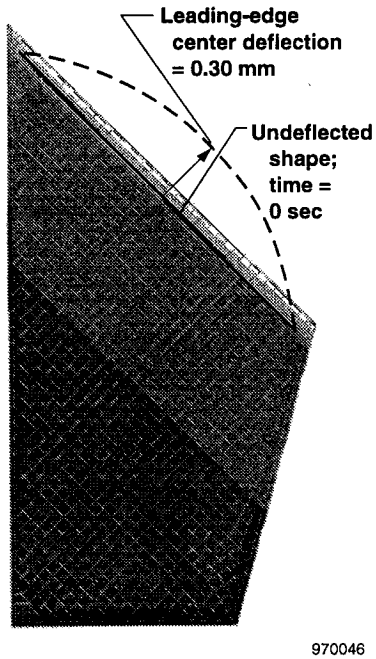

(d) Leading-edge deflection at 90 sec.

Figure 11: Leading-edge thermal displacement of wing and glove.

CONCLUDING REMARKS

A nonlinear finite-element analysis has been performed to validate a test article design for an in-flight Mach-8 aerodynamic research experiment. A nonlinear analysis was required to represent several complex design features. Complexity of the design was caused in large part by the use of a nonlinear restraint mechanism that attaches the glove to the wing of the space booster. The restraint mechanism was designed to securely attach the glove to the wing in directions normal to the wing/glove interface surface, but allow the glove to thermally expand and contract to alleviate stresses in directions parallel to the interface surface. This design allows the glove to maintain a geometrically stable shape, reduces the thermal stress in the glove to acceptable levels, and results in a safe and efficient structural design. The finite-element analysis used nonlinear contact elements to model the complex behavior of the sliding restraint mechanism. The contact elements were shown to be critical in modeling the thermal expansion and contraction of the glove during the severe temperature environment expected in the experiment. These elements allowed the thin skin on the glove to remain nearly stress-free away from the leading edge. Results show that all glove components are well within the allowable stress and deformation requirements to satisfy the objectives of the boundary-layer experiment.

REFERENCES

[1] Bertelrud, Arild, Kolodziej, Paul, Noffz, Greg K., and Godil, Afzal. "Plans for In-Flight Measurement of Hypersonic Crossflow Transition on the Pegasus® Launch Vehicle," AIAA-92-4104, Aug. 1992.

[2] Noffz, Gregory K., Curry, Robert E., Haering, Edward A., Jr., and Kolodziej, Paul. *Aerothermal Test Results From the First Flight of the Pegasus Air-Launched Space Booster*, NASA TM-4330, Oct. 1991.

[3] Noffz, Gregory K., Moes, Timothy R., Haering, Edward A., Jr., and Kolodziej, Paul. *Aerothermal Test Results From the Second Flight of the Pegasus Booster*, NASA TM-4391, Oct. 1992.

[4] Curry, Robert E., Meyer, Robert R., Jr., and Budd, Gerald D. "Pegasus Hypersonic Flight Research," SAE Technical Paper Series 921995, Oct. 1992.

[5] Richards, W. Lance and Monaghan, R. C. "Analytical and Experimental Verification of a Flight Article for a Mach-8 Boundary-Layer Experiment," *Computational Methods and Testing for Engineering Integrity*, Computational Mechanics Publications, Southampton, United Kingdom, 1996, pp. 115–130.

[6] Gong, Leslie, Richards, W. Lance, Monaghan, Richard C., and Quinn, Robert D. *Preliminary Analysis for a Mach 8 Crossflow Transition Experiment on the Pegasus® Space Booster*, NASA TM-104272, Nov. 1993.

[7] Godil, A. and Bertelrud, A. "Design of a Wing Shape for Study of Hypersonic Crossflow Transition in Flight," *Computing Systems in Engineering*, vol. 3, no. 1–4, Pergamon Press Ltd, Great Britain, 1992, pp. 115–130.

[8] Lahey, Robert S., Miller, Mark P., and Reymond, Michael (ed). *MSC/NASTRAN Reference Manual, Version 68,* vol. 1, The MacNeal-Schwendler Corporation, USA, 1994.

[9] Timoshenko, Stephen P. and Gere, James M. *Theory of Elastic Stability*, second edition, McGraw Hill Book Company Inc., New York, 1961.

[10] Lee, Sang H. (ed). *MSC/NASTRAN Handbook for Nonlinear Analysis, Version 67*, The MacNeal-Schwendler Corporation, USA, 1992.

REPORT DOCUMENTATION PAGE

Form Approved
OMB No. 0704-0188

1. AGENCY USE ONLY (Leave blank)	2. REPORT DATE	3. REPORT TYPE AND DATES COVERED
	June 1997	Technical Memorandum

4. TITLE AND SUBTITLE

Finite-Element Analysis of a Mach-8 Flight Test Article Using Nonlinear Contact Elements

5. FUNDING NUMBERS

WU 529-60-24

6. AUTHOR(S)

W. Lance Richards

7. PERFORMING ORGANIZATION NAME(S) AND ADDRESS(ES)

NASA Dryden Flight Research Center
P.O. Box 273
Edwards, California 93523-0273

8. PERFORMING ORGANIZATION REPORT NUMBER

H-2169

9. SPONSORING/MONITORING AGENCY NAME(S) AND ADDRESS(ES)

National Aeronautics and Space Administration
Washington, DC 20546-0001

10. SPONSORING/MONITORING AGENCY REPORT NUMBER

NASA TM-4796

11. SUPPLEMENTARY NOTES

Presented at the Contact Mechanics 1997 Conference, Madrid, Spain, July 1–3, 1997.

12a. DISTRIBUTION/AVAILABILITY STATEMENT

Unclassified—Unlimited
Subject Category 39

12b. DISTRIBUTION CODE

13. ABSTRACT (Maximum 200 words)

A flight test article, called a glove, is required for a Mach-8 boundary-layer experiment to be conducted on a flight mission of the air-launched Pegasus® space booster. The glove is required to provide a smooth, three-dimensional, structurally stable, aerodynamic surface and includes instrumentation to determine when and where boundary-layer transition occurs during the hypersonic flight trajectory. A restraint mechanism has been invented to attach the glove to the wing of the space booster. The restraint mechanism securely attaches the glove to the wing in directions normal to the wing/glove interface surface, but allows the glove to thermally expand and contract to alleviate stresses in directions parallel to the interface surface. A finite-element analysis has been performed using nonlinear contact elements to model the complex behavior of the sliding restraint mechanism. This paper provides an overview of the glove design and presents details of the analysis that were essential to demonstrate the flight worthiness of the wing-glove test article. Results show that all glove components are well within the allowable stress and deformation requirements to satisfy the objectives of the flight research experiment.

14. SUBJECT TERMS

Computational methods, Finite element analysis, Hypersonic flight research, Nonlinear analysis, Structural design

15. NUMBER OF PAGES

18

16. PRICE CODE

A03

17. SECURITY CLASSIFICATION OF REPORT	18. SECURITY CLASSIFICATION OF THIS PAGE	19. SECURITY CLASSIFICATION OF ABSTRACT	20. LIMITATION OF ABSTRACT
Unclassified	Unclassified	Unclassified	Unlimited